Korean J. Chem. Eng., **30**(1), 213-220 (2013)
DOI: 10.1007/s11814-012-0112-2

Correlation of density for binary mixtures of methanol+ionic liquids using back propagation artificial neural network

Mostafa Lashkarbolooki*,†, Ali Zeinolabedini Hezave*, and Aziz babapoor**

*Islamic Azad University, Dashtestan Branch, Borazjan, Iran
**Department of Chemical Engineering, Ahar Branch, Islamic Azad University, Ahar, Iran
(*Received 21 May 2012 • accepted 7 July 2012*)

Abstract−Ionic liquids (ILs) are amazing fluids introduced as a replacement for conventional solvents due to their unique properties. Unfortunately, they have several unfavorable features such as high viscosity, which makes pumping them difficult on industrial scale. In this regard, several researchers mix the ionic liquids with each other or some conventional solvents, organic and inorganic compounds, to eliminate those unfavorable features. So the binary properties of the ILs mixtures have been increasingly measured and correlated through the past years. One of the most widely used solvents and additives in the different chemical industries is methanol. In the present investigation, the capability of artificial neural networks for correlating the binary density of the ILs systems containing methanol as a common part (total of 426 experimental data points) has been examined. The results revealed that the best network architecture obtained in this study was feasible to correlate the binary densities of the ILs mixtures with average absolute relative deviation percent (AARD%), average relative deviation percent (ARD%) and correlation coefficient (R^2) values of 0.85%, −0.05 and 0.9948, respectively.

Key words: Methanol, Ionic Liquids, Binary Density, Correlation, Artificial Neural Network

INTRODUCTION

Ionic liquids (ILs) due to their unique properties have gained an increasing interest in the past ten years. ILs can be tailored to a specific application, so many researchers around the world through the academic and industrial communities have concentrated on the possible application of the ILs not only because of their amazing features, but also since they can be tailored in a way to be useful for different industries [1-9].

However, there are still several obstacles limiting the practical applications of ILs. One of the most important difficulties is that many of these compounds tend to have high viscosity. This could limit mass transfer in separations processes and increase the cost of transporting ionic liquids. It is also well-known that ionic liquids are very hygroscopic, readily absorbing water from the atmosphere. There are also studies being done that indicate that many of the popular ionic liquids may exhibit a high degree of aquatic toxicity [10-13], thereby calling into question the title of "green solvents."

In addition, purification and separation processes dealing with ILs due to their very low vapor pressure and other unique properties are not cost effective. In this regard, as a way out, it is possible to mix an ionic liquid with another ionic liquid or with certain organic solvents to overcome some of the limitations. In addition, mixing with other solvents not only can eliminate some of these difficulties effectively, but also sometimes, it is possible to gain some new favorable performance. Therefore, many studies have addressed the physicochemical properties of ionic liquid mixtures.

For example, Qian et al. [14] measured the densities and viscosities of the pure ionic liquid 1-methylimidazolium acetate ([Mim]Ac), and its binary mixtures with methanol, ethanol, 1-propanol, and 1-butanol were measured at temperature ranging from T=(293.15 to 313.15) K. in addition, Mokhtarani and coworkers [15] measured densities and viscosities of two pyridinium-based ionic liquids, 1-butylpyridinium tetrafluoroborate [BuPy][BF4] and 1-octylpyridinium tetrafluoroborate [OcPy][BF4], and their binaries with water at atmospheric pressure and temperatures from (283.15 to 348.15) K. Also, Gomez et al. [16] reported the measurement of densities, dynamic viscosities, speeds of sound, and isentropic compressibilities, which were determined over the whole composition range for ethanol (1)+1-ethyl-3-methylimidazolium ethylsulfate (2) and water (1)+1-ethyl-3ethylimidazolium ethyl sulfate (2) binary systems at T) (298.15, 313.15, and 328.15) K and atmospheric pressure. Lehmann and her colleagues [17] reported density data for binary mixtures of the ionic liquid 1-ethyl-3-methylimidazolium ethyl sulfate ([EMIM][EtSO4]) with acetone, acetonitrile, propylene carbonate, dichloromethane, methanol, ethanol and water. Wang et al. [18] measured the density for binary mixtures of water and three ionic liquids (ILs), respectively: (3-aminopropyl) tributylphosphonium L-α-aminopropionic acid salt ([aP4443][Ala]), (3-aminopropyl) tributylphosphonium l-α-aminoisovaleric acid salt ([aP4443][Val]), and (3-aminopropyl) tributylphosphonium l-α-amino-4-methylvaleric acid salt ([aP4443][Leu]). More recently, Yu and coworkers [19] reported the densities, viscosities and refractive indices for two ionic liquid+methanol formed by the 1-butyl-3-methylimidazolium glutamic acid salt ([Bmim][Glu]) or the 1-butyl-3-methylimidazolium glycine acid salt ([Bmim][Gly]), respectively, in a wide range of mole fraction and temperatures at atmospheric pressure.

It is evident that the properties of every conceivable IL and its mixture with solvents cannot be obtained by carrying out appropri-

†To whom correspondence should be addressed.
E-mail: mostafalashkarbolooki@yahoo.com

ate measurements, which is a more substantial investment. In this context, it would be helpful to predict the desired properties of an IL and its mixtures with dissolved substances in dependence on composition and temperature.

Generally, throughout the years, the computational changes have brought growth to new technologies. In this way, several predictive methods that can predict unknown values from data observed at other known locations with any degree of complexity, such as the Kriging method [20,21], the radial basis function [22], artificial neural networks etc. have been developed. Among these methods, artificial neural networks have gained popularity as feasible tools in a variety of industries due their simplicity and multi-functionality. One of the main attractions of the ANN approach is that it does not require an explicit understanding of the mechanisms underlying the process in the phenomenon studied. Instead, the ANN approach possesses the capability to learn from data sets pertaining to the process. According to this capability, artificial neural networks over the years have given various solutions to the industry. Neural networks are significantly capable to map any relationship with any complexities.

An artificial neural network is a system based on the operation of biological neural networks, that is, an emulation of a biological neural system [23]. An artificial neural network receives an input, processes the data, and provides an output. Once an input is presented to the neural network, and a corresponding desired or target response is set at the output, an error is composed from the difference of the desired response and the real system output. The error information is fed back to the system which makes all adjustments to their parameters in a systematic fashion (commonly known as the learning rule). This process is repeated until the desired output is acceptable. In any predictive tool it is crucial that the tool be flexible and be able to correlate any complex relationship. Fortunately, ANN provides these two necessities simultaneously, making it favorable as a predictive tool especially when dealing with complex relationships. In the light of these unique capabilities, ANNs have been widely used during the past decades in particular for property correlation.

ILs systems are new and amazing fluids with a wide range of applications due to their unique properties. On the other hand, those amazing and unique properties make them complex systems to be predictable. In this regards, the ionic liquids complexity and powerful correlative capability of ANNs leads to several investigations on the correlation of different properties of ionic liquids based on the ANNs modeling.

Also, in the field of ionic liquids several groups around the world have performed several studies on the application of the ANNs for correlating the properties of the ionic liquids, especially the imidazolium family. Lazzús [24] reported successful application of artificial neural network to correlate a total of 2410 data points of density at several temperatures and pressures (ρ-T-P), corresponding to 250 ionic liquids. In addition, Lazzús [24] has given molecular mass and the structure of the molecule as the input variables to discriminate between the different substances. In addition, Torrecilla et al. [25] presented an optimized artificial neural network (ANN) model for predicting the melting point of a group of 97 imidazolium salts with varied anions. Their model was able to correlate the melting point with mean prediction error of 1.30%, a regression coefficient of 0.99 and a mean P-value of 0.92. Bini and coworkers [26] reported that the recursive neural network (RNN) was an applicable tool to predict the melting points of several pyridinium-based ionic liquids (ILs). Furthermore, coauthors have previously reported that the ANNs are good tools to predict the binary heat capacity and ternary electrical conductivity of the systems containing ILs [27-30]. Miao et al. [31] used the artificial neural network (ANN) model to predict the compositional viscosity of binary mixtures of room temperature ionic liquids (in short as ILs) [Cn-mim][NTf2] with n=4, 6, 8, 10 in methanol and ethanol over the entire range of molar fraction at a broad range of temperatures from T= 293.0-328.0 K.

In short, the efficiency of ANN has already been confirmed for the prediction of not only several properties of ionic liquids but also to correlate, predict or estimate many thermodynamic properties. For example, successful applications of neural networks to predict mixture properties, such as solid solubilities in supercritical fluids, vapor liquid equilibria, and activity coefficients among others, have been published in the literature [32].

In this respect, using predictive tools, such as artificial neural network (ANN) programming to easily estimate the transport properties of pure ILs, as well as their binary and ternary mixtures, can be useful. To the best of our knowledge, there is no report on the application of the binary density correlation of the ILs mixtures using the ANN model. So, the binary density of the ILs systems containing methanol as a common part was correlated accurately by using feed forward artificial neural network (ANNs).

METHODOLOGY

As aforementioned, neural networks are a very popular data mining and data correlative tool. Their origin stems from the attempt to model the human thought process as an algorithm which can be efficiently run on a computer [33]. The human brain consists of neurons that send activation signals to each other, thereby creating intelligent thoughts. The algorithmic version of a neural network (called an artificial neural network) also consists of neurons which send activation signals to one another.

Totally, artificial neural network can approximate a function dealing with a large number of inputs and outputs. As a consequence, neural networks can be used for a variety of data mining tasks, such as classification, descriptive modeling, clustering, function approximation, and time series prediction [34]. Neural networks are composed of a large number of highly interconnected processing elements (neurons) working in parallel to solve specific problems. ANNs are able to be trained and configured for a specific application, such as pattern recognition or data classification. Due to the high flexibility and capability of the ANNs to deal with high number of parameters, ANNs have been welcomed during the past decades for different applications, in particular for properties estimation of chemical substances utilized in different chemical industries [24-30,35-42].

1. Back-propagation Algorithm

There are two kinds of mostly used types of ANNs, namely feed forward and back propagation. Without any question, back-propagation is currently the most widely applied neural network architecture. This popularity primarily revolves around the ability of back-propagation networks to learn complicated multidimensional mapping. One way to look at this ability is that, in the words of Werbos

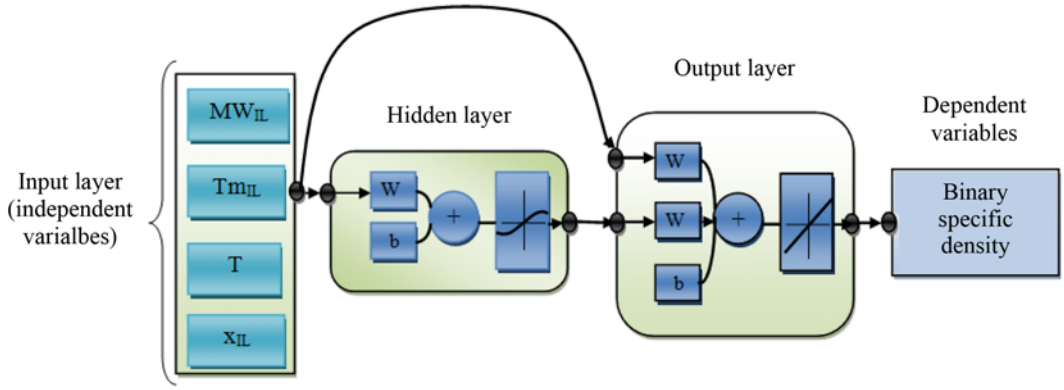

Fig. 1. Structure of the artificial neural network for binary density of ILs mixtures containing methanol.

Table 1. Determining the number of hidden layers

Number of hidden layers	Result
None	Only capable of representing linear separable functions or decisions.
1	Can approximate arbitrarily while any functions which contain a continuous mapping from one finite space to another.
2	Represent an arbitrary decision boundary to arbitrary accuracy with rational activation functions and can approximate any smooth mapping to any accuracy.

[43,44], back-propagation goes 'Beyond Regression'. Back-propagation was originally introduced by Bryson and Ho in 1969 [45] and independently rediscovered by Werbos in 1974 [46], by Parker in the mid 1980's [47,48] and by Rumelhart, Williams and other members of the PDP group in 1985 [49,50]. A simple schematic of the used back-propagation artificial neural network is shown in Fig. 1.

2. Back-propagation Training and Testing

In the employment of the back-propagation algorithm, each iteration of training involves the following steps: 1) a particular case of training data is fed through the network in a forward direction, producing results at the output layer, 2) error is calculated at the output nodes based on known target information, and the necessary changes to the weights that lead into the output layer are determined based upon this error calculation, 3) the changes to the weights that lead to the preceding network layers are determined as a function of the properties of the neurons to which they directly connect (weight changes are calculated, layer by layer, as a function of the errors determined for all subsequent layers, working backward toward the input layer) until all necessary weight changes are calculated for the entire network. The calculated weight changes are then implemented throughout the network, the next iteration begins, and the entire procedure is repeated using the next training pattern. In the case of a neural network with hidden layers, the back-propagation algorithm is given by the following three equations (modified after Gallant [51]), where i is the "emitting" or "preceding" layer of nodes, j is the "receiving" or "subsequent" layer of nodes, k is the layer of nodes that follows j (if such a layer exists for the case at hand), ij is the layer of weights between node layers i and j, jk is the layer of weights between node layers j and k, weights are specified by w, node activations are specified by a, delta values for nodes are specified by d, subscripts refer to particular layers of nodes (i, j, k) or weights (ij, jk), "sub-subscripts" refer to individual weights and nodes in their respective layers, and epsilon is the learning rate:

$$\Delta w_{ij_m} = \varepsilon \delta_{j_p} a_{i_q} \quad (1)$$

$$\delta_{j_p} = a_{j_p}(1-a_{j_p})(t_{j_p}-a_{j_p}) \text{ (for output neurons)} \quad (2)$$

$$\delta_{j_p} = a_{j_p}(1-a_{j_p})\sum \delta_{k_x} w_{jk_x} \text{ (for intermediate neurons)} \quad (3)$$

In addition, similar to the conventional feed forward artificial neural networks, the activation functions, number of neurons in the hidden layer and number of hidden layers must be optimized.

Although, it is possible to consider different numbers of hidden layers through the network due to the potential of each number hidden layers (see Table 1). But, in this study, a network with only one hidden layer was proposed since Cybenko [52] claimed that a network with only one hidden layer is able to correlate any complexities.

In the first stage, the collected binary density of the ILs mixtures containing methanol from the different previously published literature [53-61] were divided into two different subsets including training (data points) and testing (data points) data subsets. The point that must be clarified here is that it is possible to have available several experimental data sets for some cases. For example, there were three reported sets of experimental data points on the binary density of the methanol+1-butyl-3-methylimidazolium tetrafluoroborate [54-56]. The difference between these reported data points may rise from the measurement techniques or the purity of the used samples. By the way, because there was no convenient reason to decide which set of measured experimental binary densities are the best, all of the reported measurements ignoring their accuracy were used.

In the training stage, Levenberg-Marquardt (LM) [62] optimization algorithm and the average absolute relative deviation percent (AARD%, see Eq. (4)) as the objective function were used to optimize the network parameters. The point that should be considered is that the collected data, which were randomly divided into two subsets, namely the training and testing data subsets, were selected

Table 2. The physiochemical properties of IL compounds used in this study

Compounds	MW	Tm (K)
1-Butyl-3-methylimidazolium hexafluorophosphate	283.15	284.18
1-Butyl-3-methylimidazolium tetrafluoroborate	192.15	226.03
1-Methyl-3-octylimidazolium tetrafluoroborate	193.15	282.13
1-Butyl-3-methylimidazolium chloride	314.15	174.67
1-Methyl-3-octylimidazolium chloride	285.41	230.78
1-Ethyl-3-methylimidazolium trifluoromethanesulfonate	264.15	260.24
1-Butyl-3-methylimidazolium methylsulfate	253.15	250.31

in a way that covered all the range of the experimental conditions, since the ANN approach is a correlative method. In addition, for better interpretation of the obtained results, other statistical parameters including average relative deviation percent (ARD%), minimum relative deviation (RD_{min}), maximum relative deviation (RD_{max}) and correlation coefficient (R2) were utilized (see Eq. (5)-(7)):

$$AARD\% = \frac{1}{N}\sum\left(\left|\frac{\rho_i^{exp.} - \rho_i^{cal.}}{\rho_i^{exp.}}\right|\right) \times 100 \quad (4)$$

$$RD\% = (\rho^{exp} - \rho^{cal}/\rho^{exp}) \times 100 \quad (5)$$

$$R^2 = \frac{\sum_i^N (\rho_i^{exp.} - \overline{\rho})^2 - \sum_i^N (\rho_i^{exp.} - \rho_i^{cal.})^2}{\sum_i^N (\rho_i^{exp.} - \overline{\rho})^2} \quad (6)$$

$$ARD\% = \frac{1}{N}\sum(\rho^{exp} - \rho^{cal}/\rho^{exp}) \times 100 \quad (7)$$

where N is the number of binary densities, ρ_i^{exp} is the experimental binary density; ρ_i^{cal} is the calculated binary density and $\overline{\rho}$ is the average value of the binary density.

The training data set was selected in a way which covers all the IL composition and temperature ranges of the investigated binary systems. In the training stage, using a trial and error approach, the number of neurons in the hidden layer and transfer functions of the hidden and output layers was obtained. In the light of using trial and error approach, the number of the neurons in the hidden layer started from a small number of neurons. Then, the number of neurons in the hidden layer increased continuously and the obtained AARD% of the training and testing stages was recorded. Finally, based on the smallest obtained AARD% for the testing data subset, the number of neurons in the hidden layer was selected.

The point that should be explained is that the chemicals used through the modeling must be defined to the network. In other words, some properties of the chemicals including melting point temperature and molar mass (see Table 2) were used to discriminate among the different compounds. In addition, the ILs composition and temperature were introduced to the network to differentiate between the different binary systems. In summary, in the present study, the functionality of the binary density of ILs mixtures containing methanol was considered as below:

$$\rho = f(x_{IL}, T_{system}, T_m, Mw) \quad (8)$$

The points that should be clarified about the selection of compositions, molar mass and melting point as the input variables are:

- Defining the involved substances to the network: the network needs some specifications to differentiate the different involved substances. In this direction, molar mass and boiling point were used as the parameters to discriminate between the substances involved.
- Defining the different systems regarding compositions: there are different parameters which can lead to different systems including pressure, temperature and different compositions. In the present study, the effect of temperature and pressure was not considered, so only the different compositions can lead to having different systems; in this regard, the compositions were considered as the input variables to discriminate between the different systems involved.

Finally, what should not be forgotten is that, because of different reported melting points for one specific IL, the melting point which has been reported more times by different researchers or that has the higher purity was selected for the network optimization. For example, there were three reported melting points for 1-ethyl-3-methylimidazoliumtrifluoro-methanesulfonate, 263 K [63], 264 K [64] and 264.15 K [65-67], from which the third one was selected because it was reported three times with three different groups of researchers.

RESULTS AND DISCUSSION

We proposed the back-propagation neural network to correlate the binary density of the ILs mixtures containing methanol. In this direction, a network with three layers namely input, hidden and out-

Table 3. Results of topology studies to find the optimal ANN configuration

Hidden neuron		Error analysis	
		AARD%	R^2
5	Train	3.28	0.8965
	Test	3.65	0.8875
6	Train	1.80	0.9757
	Test	1.96	0.9734
7	Train	1.15	0.9835
	Test	1.03	0.9896
8	Train	0.85	0.9948
	Test	0.88	0.9948
9	Train	0.83	0.9964
	Test	1.09	0.9916
10	Train	0.81	0.9937
	Test	1.01	0.9912

Table 4. The optimum values of the weights and biases of back-propagation neural network

Neuron	Hidden layer					Output layer	
	Weights (w_{ij})[a]				Biases	Weight	Bias
	Tm_{IL}	MW_{IL}	T	x_{IL}	b_j	w_{jk}[b]	b_k
1	−27.052	−132.996	142.598	−94.941	10.789	0.494	−1122.215
2	0.005	0.006	−0.001	−3.050	−3.990	−3344.797	
3	0.160	−0.331	0.002	−1.265	43.647	−157.584	
4	−14.198	8.254	3.655	570.731	305.048	21.523	
5	1.610	37.316	−27.630	1051.971	−566.716	−8.307	
6	−5.088	3.335	0.000	3.918	225.457	1487.381	
7	−31.490	8.744	15.664	−383.073	13.086	−1731.088	
8	34.517	24.715	−42.925	−233.485	3.387	−47.264	
w_{ik}[c]	−2.425	−0.956	−1.062	35.281			

[a]Weight connection from the input layer to hidden layer
[b]Weight connection from the hidden layer to output layer
[c]Weight connection from the input layer to output layer

put was utilized. Since one hidden layer is able to correlate any relation with any complexity [52], the proposed network consisted of only one hidden layer. After that, using training and testing data sets, the weights, biases, number of neurons in the hidden layer and transfer functions were optimized. The obtained results revealed that using eight neurons in the hidden layer along the *logsig* and *purelin* as the hidden and output layers transfer functions leads to the lowest AARD% (0.88%) for the testing data set.

The error analysis results of the different numbers of the neurons in the hidden layer are listed in Table 3. In addition, the obtained weights and biases values given through Table 4 enable anyone to use the proposed network for any arbitrary binary mixtures of ILs containing methanol as the common part.

The general results of the correlated binary densities using training and testing data subsets are shown in Figs. 2 and 3. In these figures, the solid 45° line illustrates the exact fit between the experimental binary densities and correlated ones, while triangles reveal the real correlated binary densities using the proposed ANN model compared to the experimental ones. Fig. 2, which gives the correlated binary densities versus experimental ones during the training stage, reveals a good agreement between the correlated densities and experimental ones. In addition, the results of the testing stage, which correlated the densities, were not considered during the training stage, which also demonstrated the good capability of the proposed network to well correlate the binary densities of the ILs mixtures containing methanol (see Fig. 3).

Also, the correlated binary densities of several systems are given through Figs. 4 and 5 for better demonstration of the correlative capability of the proposed ANN model. It is completely obvious from Figs. 4 and 5 that the proposed correlation not only is able to well correlate the binary densities with low AARD% and ARD%, but also it is able to map the behavior of the binary densities variation along with the temperature and IL composition with a good agreement.

As it is clear in Figs. 4 and 5, any density fluctuation with IL composition and temperature is well followed by the correlated values

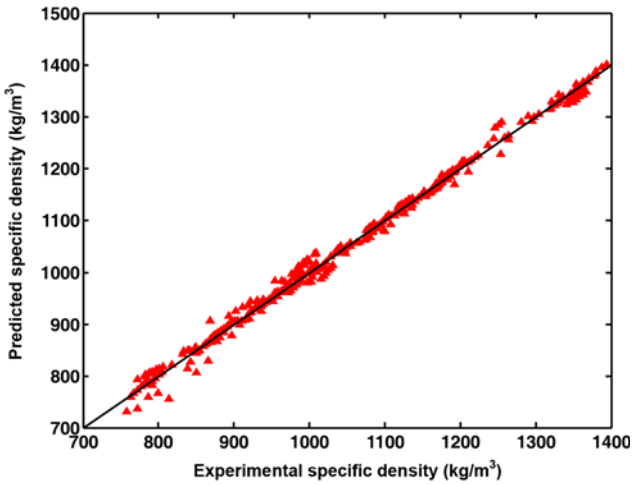

Fig. 2. Plot of experimental specific density data vs. developed ANN prediction for training.

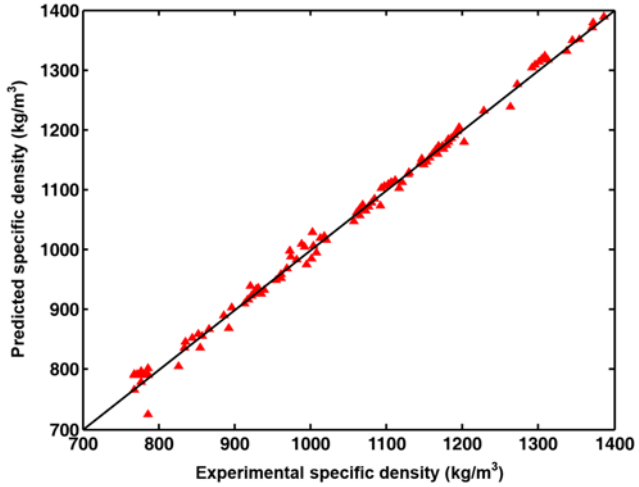

Fig. 3. Plot of experimental specific density data vs. developed ANN prediction for testing.

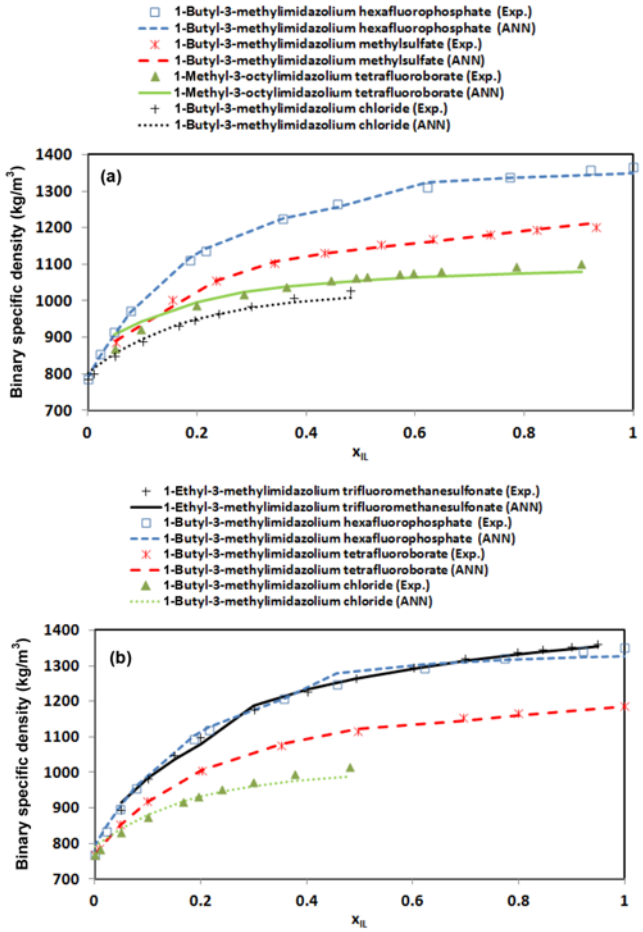

Fig. 4. The correlated binary density of several binary systems at different temperatures, (a) 298.15 K and (b) 318.15 K.

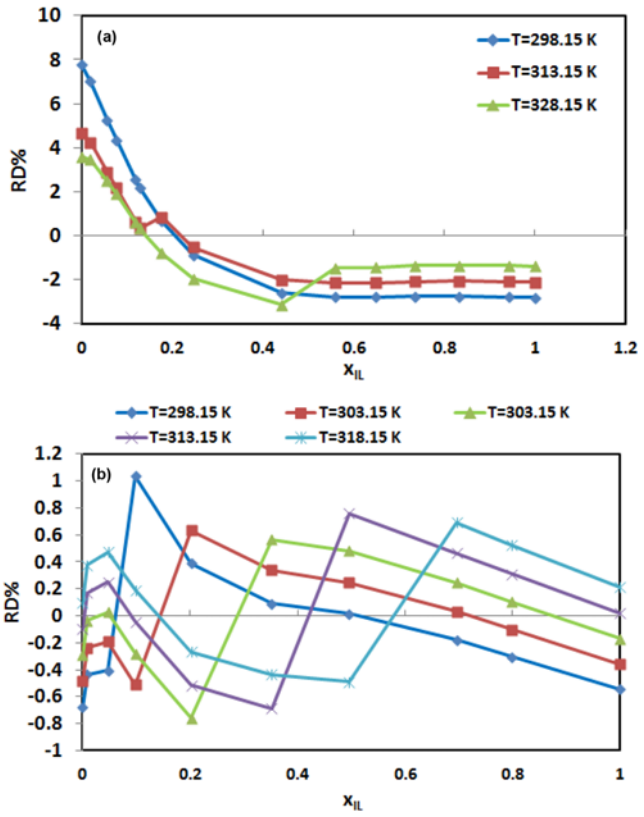

Fig. 5. Relative deviation plot of binary densities of two different binary systems, (a) 1-methyl-3-octylimidazolium chloride and (b) 1-butyl-3-methylimidazolium tetrafluoroborate.

via ANN model. In other words, it is not important how scattered are the experimental data points in both training and testing stages, ANN is able to well correlate any relation among the densities, compositions and other effective parameters. In more detail, one can observe in Fig. 4 that 1-methyl-3-octylimidazolium chloride density at temperature of 328.15 K experienced a trend variation in composition near to 0.6, but this unusual behavior cannot confuse the ANN correlating capability and the proposed ANN followed this trend with acceptable accuracy.

In addition, for 1-butyl-3-methylimidazolium tetrafluoroborate (Fig. 5) one can observe highly fluctuating density data points, while the ANN can easily map this unusual trend with an acceptable level of engineering.

Table 5. AARD%, ARD% , RD_{min}, RD_{max} and R^2 for the binary densities of ILs mixtures containing methanol as the common part at different conditions

Component IL	Temperature range (K)	x_{IL} range	N[a]	R	Error analyses				
					ARD%	AARD%	Min (RD)%	Max (RD)%	R^2
1-Butyl-3-methylimidazolium hexafluorophosphate	298.15-318.15	0-1	60	[43]	−0.33	0.90	−3.23	1.69	0.9957
1-Butyl-3-methylimidazolium tetrafluoroborate	298.15-318.15	0-1	50	[44]	0.00	0.35	−0.76	1.04	0.9992
	293.15-323.15	0-1	112	[45]	0.00	0.38	−0.90	1.24	0.9984
	298.15	0.08-0.56	11	[46]	0.11	0.41	−0.49	1.13	0.9982
1-Methyl-3-octylimidazolium tetrafluoroborate	298.15	0.05-0.90	13	[47]	0.06	1.34	−4.36	2.00	0.9383
1-Butyl-3-methylimidazolium chloride	293.15-318.15	0-0.48	60	[48]	−0.17	1.12	−3.11	2.69	0.9767
1-Methyl-3-octylimidazolium chloride	298.15-328.15	0-1	45	[49]	0.18	2.39	−3.14	7.78	0.8884
1-Ethyl-3-methylimidazolium trifluoromethanesulfonate	278.15-318.15	0.05-0.95	65	[50]	−0.02	0.73	−2.61	2.19	0.9946
1-Butyl-3-methylimidazolium methylsulfate	298.15	0.05-0.94	10	[51]	0.15	0.52	−0.88	1.99	0.9931
Overall	278.15-328-15	0-1	426		−0.05	0.85	−4.36	7.78	0.9948

[a]Number of data

In addition, the results for every binary system are listed in Table 4 in more details, enabling anyone to observe the correlative capability of the proposed ANN model for all of the involved binary systems. It is completely obvious that the overall AARD% is 0.85%, which demonstrates the high capability of the proposed ANN model for binary density correlation. But the more important point is that considering the obtained results and the reported uncertainties through the literatures, from which the experimental data were extracted, leads to this conclusion that the proposed ANN model is able to accurately predict the binary densities with enough reliability since the AARD% due to the experimental uncertainties were smaller than those obtained from the correlated binary densities. In general, it can be concluded that the ANN model is applicable and feasible to well correlate the complex binary system properties, in particular density, of the ILs containing methanol as the common part.

CONCLUSION

The capability and feasibility of back-propagation artificial neural network has been examined through 426 binary density data point collected from the different published literatures. In the first step, the collected data bank was divided into two different data sets, namely training and testing sets. The training set was used to train the proposed network and find the optimum network parameters including weights, biases, number of neurons in the hidden layer and transfer functions through the hidden and output layers.

Applying trial and error approach leads to selection of eight neurons in one hidden layer besides the *logsig* and *purelin* transfer functions for the hidden and output layers, respectively, since causes AARD% of 0.85%. After that, the trained network was tested with about one-fourth of the collected data not examined in the training stage. The obtained error analysis results showed a low AARD% of 0.88%. Then, the optimum values of the weights and biases enable anyone to repeat and recalculate the correlated binary densities through this study were reported in the section under the heading of "Results and discussions".

These reported fitted parameters enable one to not only repeat all the calculations but also to correlate the binary density of systems containing methanol as the common part. Furthermore, error analysis results revealed that the proposed ANN model was able to correlate the binary densities with AARD% of 0.85%, which means a rather good correlative capability. In addition, the obtained correlation coefficient (R^2), which is in the range of 0.8884-0.9992, shows an acceptable level of correlative capability of the trained and tested artificial neural network. Also, considering all the reported results it is completely obvious that the accuracy of the used ANN is enhanced if larger amount of data is fed to the system. Generally, the results obtained for 1-butyl-3-methylimidazolium tetrafluoroborate+ methanol with total reported experimental data of 173 were 0.38% while the other system experiences higher deviations. According to these obtained results, the proposed ANN model is highly capable to correlate the density of complex systems containing ionic liquids and methanol as the common part.

REFERENCES

1. A. Balducci, F. Soavi and M. Mastragostino, *Appl. Phys. A: Mater. Sci. Process*., **82**, 627 (2006).
2. M. E. Van Valkenburg, R. L. Vaughn, M. Williams and J. S. Wilkes, *Thermochim. Acta*, **425**, 181 (2005).
3. T. Welton, *Chem. Rev.*, **99**, 2071 (1999).
4. J. Dupont, R. F. de Souza and P. A. Z. Suarez, *Chem. Rev.*, **102**, 3667 (2002).
5. J. S. Wilkes, Ionic Liquids in Perspective: The Past with an Eye toward the Industrial Future. In Ionic Liquids: Industrial Applications for Green Chemistry; Rogers, D., Seddon, K. R., Eds.; ACS Symposium Series 818; American Chemical Society: Washington, DC, 214 (2002).
6. K. Schroer, E. Tacha and S. Lutz, *Org. Process Res. Dev.*, **11**, 836 (2007).
7. H. K. Farag and F. Endres, *J. Mater. Chem*., **18**, 442 (2008).
8. N. Birbilis, P. C. Howlett, D. R. MacFarlane and M. Forsyth, *Surf. Coat. Technol*., **201**, 4496 (2007).
9. T. Fukushima and T. Aida, *Chem. Eur. J*., **13**, 5048 (2007).
10. K. M. Docherty and C. F. Kulpa, *Green Chem*., **7**, 185 (2005).
11. R. J. Bernot, M. A. Brueseke, M. A. Evans-White and G. A. Lamberti, *Environ. Toxicol. Chem*., **24**, 87 (2005).
12. R. P. Swatloski, J. D. Holbrey, S. B. Memon, G. A. Caldwell, K. A. Caldwell and R. D. Rogers, *Chem. Commun*., 668 (2004).
13. R. P. Swatloski, J. D. Holbrey and R. D. Rogers, *Green Chem*., **5**, 361 (2003).
14. W. Qian, Y. Xu, H. Zh and C. Yu, *J. Chem. Thermodyn.*, **49**, 87 (2012).
15. B. Mokhtarani, A. Sharifi, H. R. Mortaheb, M. Mirzaei, M. Mafi and F. Sadeghian, *J. Chem. Thermodyn.*, **41**, 323 (2009).
16. E. Gomez, B. Gonzalez, N. Calvar, E. Tojo and A. Domınguez, *Chem. Eng. Data*, **51**, 2096 (2006).
17. M. H. Rausch, A. Leipertz, A. P. Froba and J. Lehmann, *J. Chem. Eng. Data*, **55**, 4068 (2010).
18. H. Xu, Y. Shang, L. Zhang, J. Zhang, Z. Wang and L. Fu, *J. Chem. Eng. Data*, **57**(4), 1057 (2012).
19. Z. Yu, H. Gao, H. Wang and L. Chen, *J. Sol. Chem*., **41**(1), 173 (2012).
20. E. Davis and M. Ierapetritou, *AIChE J*., **53**(8), 2001 (2007).
21. M. A. Oliver and R. Webster, *INT. J. Geographical Information Systems*, **4**(3), 313 (1990).
22. J. Moody and C. J. Darken, *Neural Compu*., **1**, 281 (1989).
23. http://www.learnartificialneuralnetworks.com/.
24. J. A. Lazzús, *J. Taiwan Inst. Chem. Eng*., **40**, 213 (2009).
25. J. S. Torrecilla, F. Rodríguez, J. L. Bravo, G. Rothenberg, K. R. Seddon and I. López-Martin, *Phys. Chem. Chem. Phys*., **14**, 5826 (2008).
26. R. Bini, C. Chiappe, C. Duce, A. Micheli, R. Solaro, A. Starita and M. R. Tiné, *Green Chem*., **10**, 306 (2008).
27. M. Lashkarbolooki, A. Z. Hezave and S. Ayatollahi, *Fluid Phase Equilib*., **324**(25), 128 (2012).
28. A. Z. Hezave, M. Lashkarbolooki and S. Raeissi, *Fluid Phase Equilib*., **314**, 128 (2012).
29. M. Lashkarbolooki, A. Z. Hezave, A. M. Al-Ajmi and S. Ayatollahi, *Fluid Phase Equilib*., **326**(25), 15 (2012).
30. A. Z. Hezave, M. Lashkarbolooki and S. Raeissi, *Ind. Eng. Chem. Res*., In Press (2012).
31. Y. Miao, Q. Gan and D. Rooney, *IEEE*, 668 (2010).
32. IUPAC Ionic Liquids Database-(ILThermo), NIST Standard Reference Database.

33. K. Watanabe, L. Matsuura, M. Abe and M. Kubota, *AIChE J.*, **35**, 1803 (1989).
34. http://www.emilstefanov.net/Projects/NeuralNetworks.aspx.
35. A. Sözen, E. Arcaklioğlu, T. Menlik and M. Özalp, *Expert Syst. Appl.*, **36**, 4346 (2009).
36. A. Sözen, M. Özalp and E. Arcaklioğlu, *Chem. Eng. Process.*, **43**, 1253 (2004).
37. R. Eslamloueyan and M. H. Khademi, *Chemometr. Intell. Lab.*, **104**, 195 (2010).
38. R. Eslamloueyan and M. H. Khademi, *Int. J. Therm. Sci.*, **48**, 1094 (2009).
39. M. Lashkarbolooki, A. Z. Hezave and S. Ayatollahi, *Fluid Phase Equilib.*, In Press (2012).
40. S. Laugier and D. Richon, *Fluid Phase Equilib.*, **210**, 247 (2003).
41. R. Eslamloueyan and M. H. Khademi, *J. Chem. Eng. Data*, **54**, 922 (2009).
42. R. Boozarjomehri, F. Abdolahi and M. A. Moosavian, *Fluid Phase Equilib.*, **231**, 188 (2005).
43. P. J. Werbos, Back-propagation: Past and Future, Proc. 1988 IEEE International Conference on Neural Neiworks, IEEE Press, New York (1988).
44. P. J. Werbos, Building and Understanding Adaptive Systems: A Statistical/Numerical Approach to Factory Automation and brain Research, IEEE Trans. On Systems, Man and Cyber. SMC-17, No. 1, 7-20, January/February (1987).
45. A. E. Bryson and Y. C. Ho, *Applied optimal control*, Blaisdell, New York (1969).
46. P. J. Werbos, Beyond Regression: New Tools for Prediction and Analysis in the Behavioral Sciences, Ph. D Thesis, Applied Mathematics, Harvard University, November (1974).
47. D. B. Parker, Learning-Logic, Technical Report TR-47, Center for Computational Research in Economics and Managernent Science, MIT, April (1985).
48. D. B. Parker, *Optimal algorithms for adaptive networks: Second order back propagation, Second order direct propagation, and second order hebbian learning, Proc.* 1987 IEEE International Conference on Neural Networks, II (593-600), IEEE Press, New York (1987).
49. J. A. Anderson, E. Ftosenfeld, [Eds.], *Neurocomputing: Foundations of Research*, MIT Press, Cambridge, Massachusetts (1988).
50. D. E. Rumelhart, G. E. Hinton and R. J. William, *Nature*, **323**, 533 (1986).
51. S. I. Gallant, Neural Network Learning and Expert Systems, MIT Press, Cambridge (1993).
52. G. V. Cybenko, *Math. Contr. Signals Syst.*, **2**, 303 (1989).
53. M. T. Zafarani-Moattar and H. Shekaari, *J. Chem. Eng. Data*, **50**, 1694 (2005).
54. M. T. Zafarani-Moattar and H. Shekaari, *J. Chem. Thermodyn.*, **38**(11), 1377 (2006).
55. M. A. Iglesias-Otero, J. Troncoso and E. Carballo, *J. Solution Chem.*, **36**, 1219 (2007).
56. A. Stoppa, J. Hunger and R. Buchner, *J. Chem. Eng. Data*, **54**, 472 (2009).
57. A. Arce, H. Rodriguez and A. Soto, *Fluid Phase Equilib.*, **242**(2), 164 (2006).
58. Q. Yang, H. Zhang, B. Su, Y. Yang, Q. Ren and H. Xing, *J. Chem. Eng. Data*, **55**(4), 1745 (2010).
59. E. J. Gonzalez, L. Alonso and A. Dominguez, *J. Chem. Eng. Data*, **51**, 1446 (2006).
60. E. Vercher, A. V. Orchilles, P. J. Miguel and A. Martinez-Andreu, *J. Chem. Eng. Data*, **52**, 1468 (2007).
61. U. Domanska, A. Pobudkowska and A. Wisniewska, *J. Solution Chem.*, **35**(3), 311 (2006).
62. M. T. Hagan, H. B. Demuth and M. H. Beale, *Neural Network Design*, International Thomson Publishing: Boston (2002).
63. E. I. Cooper and E. J. M. O'Sullivan, New, Stable, Ambient-Temperature Molten Salts, in Gale, R. J., Blomgren, G. & Kojima, H., Proceedings of the Eighth International Symposium on Molten Salts, The Electrochemical Society, Inc., Pennington, NJ, PV, 92-16 (1992).
64. P. Bonhte, A.-P. Dias, N. Papageorgiou, K. Kalyanasundaram and M. Grätzel, *Inorg. Chem.*, **35**, 1168 (1996).
65. A. Berthod, M. J. Ruiz-Angel and S. Carda-Broch, *J. Chromatogr. A*, **1184**, 6 (2008).
66. R. Sheldon, *Catalytic reactions in ionic liquids*, *Chem. Commun.*, 2399 (2011).
67. S. H. Lee and S. B. Lee, *Chem. Commun.*, 3469 (2005).